5TH INTERNATIONAL SUPERCONDUCTIVE ELECTRONICS CONFERENCE (ISEC '95) 11-44
September 18-21, 1995 Nagoya, Japan

High-Power, High-Frequency Oscillators using Distributed Josephson-Junction Arrays

P. A. A. Booi and S. P. Benz
National Institute of Standards and Technology, Boulder, CO 80303

Abstract— We present experimental results showing emission that is coupled from distributed series arrays of wide, resistively shunted tunnel junctions to on-chip 50 Ω loads. We have detected power output of 0.85 mW at 240 GHz and power >100 μW at most frequencies in the range 100-300 GHz.

I. Introduction

Josephson junctions are voltage-tunable oscillators with characteristic frequencies in the gigahertz range. For off-chip applications above 300 GHz, high power, >1 mW coupled to 50 Ω loads, is required in order to compete with (multiplied) Gunn oscillators [1]. One-dimensional (1-D) arrays [2]-[4] and two-dimensional (2-D) arrays [5]-[9] are theoretically capable of delivering such power.

The performance of arrays of N resistively shunted tunnel junctions is limited by the junction capacitance C and the parasitic inductance L associated with the shunt resistor R [9]. The dynamics of a single junction have been shown to be unstable for large inductance parameter $\beta_L = 2\pi L I_c/\Phi_0$ [10], where I_c is the critical current and $\Phi_0 = h/2e$ is the magnetic-flux quantum. For small β_L (< 0.7) and any $\beta_c = 2\pi I_c R^2 C/\Phi_0 = (f_c/f_p)^2$, or $\beta_L < 1$ and $0.5 < \beta_c < 1$, stable period-1 oscillations exist at all voltages. $f_c = I_c R/\Phi_0$ is the characteristic frequency, and $f_p = \sqrt{I_c/2\pi C\Phi_0}$ is the plasma frequency. In experiments with 2-D arrays [9], we found that arrays emit significant coherent power for operating frequencies f_{op} in the range from f_c to the LC-resonance frequency $f_{LC} = 1/2\pi\sqrt{LC}$.

Our oscillator designs use distributed series arrays of 82 μm-wide, overdamped Nb/Al-AlO$_x$/Nb junctions that are *in situ* deposited on top of an 85 μm-wide PdAu resistor film; etched slots in the Nb base-electrode then define the shunt resistor length. This scheme allows the fabrication of resistors with a length $l_r \approx 1.5$ μm while minimizing the extra inductance that arises from Nb wires to the resistors. If the wide junction is divided into a large number of smaller junctions (in parallel), a 2-D array is created with smaller I_c and C while L is increased due to spreading of current from the junctions to the (shared) resistor. Such a 2-D array can be useful for operation at higher f_{op} due to higher f_{LC}, but will deliver considerably lower power levels than its 1-D counterpart. Since the stability of 2-D arrays is similar to that of 1-D arrays, except in arrays with large junction nonuniformity [11], [12], we have focused on 1-D arrays for high-power generation.

In this article, we present experimental results on arrays that have delivered power as high as 0.85 mW to ~50 Ω loads near 240 GHz. These arrays are tunable up to ~300 GHz and deliver power >100 μW at most frequencies in the 100-300 GHz range [13], [14].

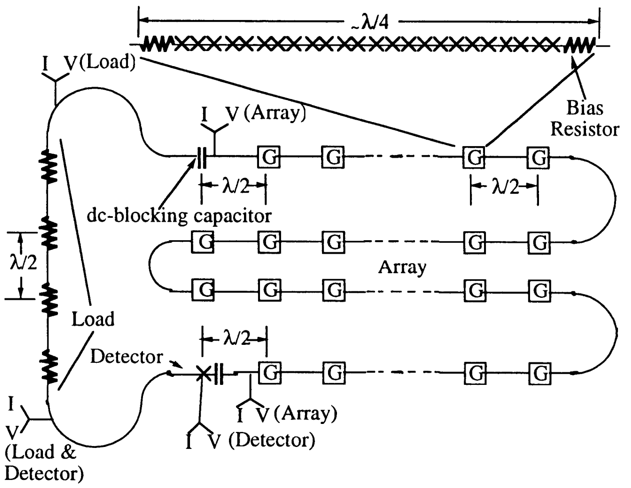

Fig. 1: Circuit schematic for the on-chip detection of emission from distributed arrays, where 'G' denotes a group of junctions and the crosses denote junctions.

II. Arrays of Wide Junctions

Design criteria for these arrays are discussed in [13]. We have designed arrays that make use of relatively low critical-current density J_c = 8-14 kA/cm^2 ($f_p \approx$ 250-320 GHz) and relatively large junction length l_j = 1.4-2 μm so that f_{LC} = 250-350 GHz and β_L = 0.6-1.2. We have limited the width of the resistors w_{RS} (and thereby the junction width w_j) and all circuit elements to 84 μm (w_j = 82 μm). With a PdAu-sheet resistance R_s = 1.1 Ω, we obtain $f_c \approx$ 120-220 GHz, so the junctions are overdamped and the current-voltage (I-V) curves are nonhysteretic.

Figure 1 shows a circuit schematic for the on-chip detection of array emission. All circuit elements are connected in series in a loop above a superconductive ground plane (GP) and are placed at the antinodes of the standing-wave mode at f_{op} where the amplitude of the rf current I_{rf} is maximal. As the circuits do not fit in a

This research is supported in part by the Office of Naval Research.

straight line on the 1 cm × 1 cm chips, we have used three 180° turns and two 90° turns with a radius $\geq 3w_{RS}$. The dc-blocking stripline capacitors on either end of the array have a length of 48 μm and a capacitance of ~0.6 pF and allow independent I-V measurements of array and detector. The load resistors have $R_s = 10\ \Omega$ (~35 nm-thick PdAu). The detector junction (which is identical to the array junctions) is placed in series with the load so that I_{rf} (through a comparison of measured and simulated I-V curves with a Shapiro step having height I_1 at voltage V_{step}) and thereby the power dissipated in the load $P_{det} = I_{rf}^2 R_L/2$ is estimated.

Bias resistors are used to force uniform current flow through the detector junction (this bias resistor is not shown in Fig. 1) and each group of junctions in the arrays. 24 junctions are lumped within 152 μm. We have used two different junction-group spacings s of 272 μm (array type A) and 340 μm (array type B). These spacings correspond to $\lambda/2$ at f_{op}, where λ is the radiation wavelength at f_{op}. Note that the ground-plane-isolating SiO_2 layer can be used to tune f_{op} once the spacings are fixed, and that w_{RS} equals 0.156 λ for array type A and 0.125 λ for array type B. For type-A (B) arrays, the load is divided into 4 (3) lumped pieces. The circuits are designed so that the total circuit length l_{cir} (and each stripline turn) equals an even (integer) number of junction-group spacings. Circuits based on type-A and type-B arrays in Fig. 1 have $l_{cir} = 31.552$ mm ($N = 1968$) and 33.32 mm ($N = 1872$) and have standing wave resonances at multiples of $f_{op}/58$ and $f_{op}/49$, respectively.

III. Results and Discussion

Spatial modulation of I_{rf} in the junction groups gives rise to a reduction of the emitted power (which is described by the factor p) that an array can generate at f_{op}:

$$P_{th} = \frac{p(v_1 N I_c R)^2 R_L}{2(NR+R_s^T+R_b+R_L)^2}, \qquad (1)$$

where v_1 is the amplitude of the fundamental junction oscillations normalized to $I_c R$. v_1 can be estimated with the approximations described in [12]. $R_b = 2.5$ (A) or 4 Ω (B) are the sums of all bias resistances for the two arrays, and R_s^T represents the total rf conductor losses in the circuit. Therefore, the choice of the number of junctions in lumped groups is a trade off between p and R_s^T. The maximum power transfer now occurs when $R_L = NR+R_s^T+R_b$ (instead of $R_L = NR$), and the power equals

$$P_{th} = \frac{p(v_1 I_c)^2 R_L}{8} (NR/R_L)^2. \qquad (2)$$

The factor p can be estimated by assuming that junction i situated at a distance x_i from a group's center will contribute $v_1 I_c \cos(\pi x_i/s)$ to the rf current at f_{op}. We determined p to be 0.77 and 0.85 for array types A and B, respectively. At frequencies f different from f_{op}, the arrays may deliver significant power, but p is considerably smaller depending on the standing wave mode.

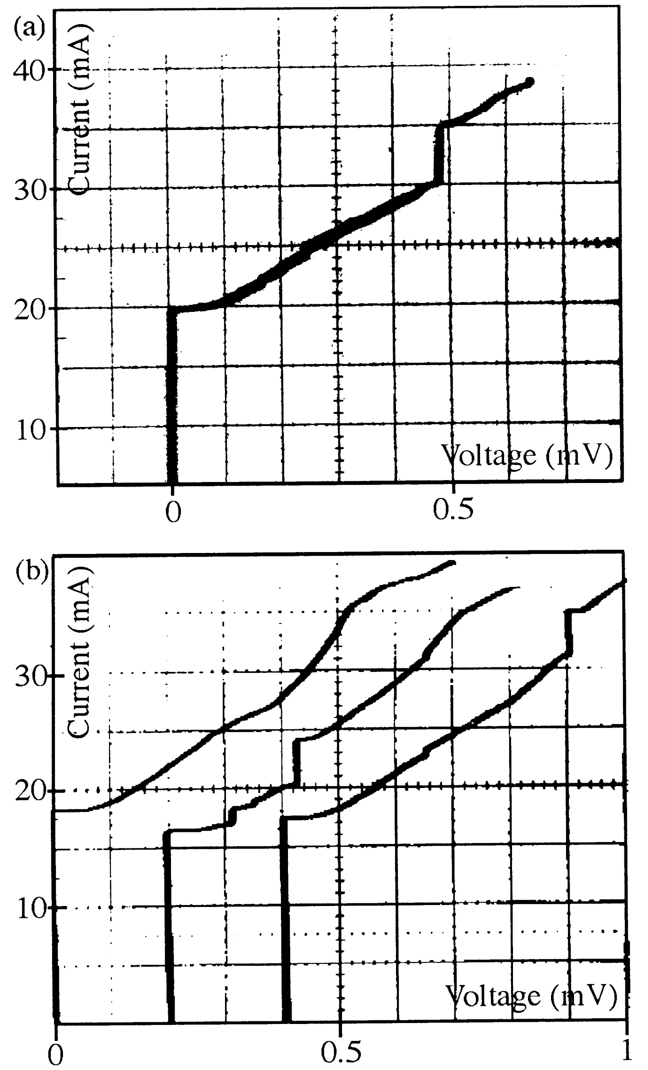

Fig. 2: I-V curves of (a) a detector under array-A1 irradiation, and (b) of a detector without array-B2 irradiation, with radiation at 115 GHz, and with irradiation at $f_{op} = 240$ GHz. Each subsequent curve in (b) has a 200 μV offset.

At low frequencies, arrays with fewer junctions and fewer stripline turns than type-A and type-B arrays show distinct stable resonant steps in their I-V curves. The high-resistance arrays with more junctions and more stripline turns, on the other hand, show switching which indicates that not just one circuit resonance is stable. This may be related to the high dynamic resistance of the array for $f < f_c$, uncertainties in the length of the stripline turns, or high β_L. This behavior is observed in the detector I-V curves as switching between Shapiro steps with different heights and sometimes different voltages (frequencies).

For frequencies near $f_{op}/3$ for type-A arrays, and near

$f_{op}/2$ for type-B arrays, switching reduces and one can observe significant coherent emission, resulting in stable 1-2 mA Shapiro steps. Local maxima in the emitted power are observed near $f_{op}/3$, $2f_{op}/3$, and f_{op} for type-A arrays, and near $f_{op}/2$ and f_{op} for type-B arrays. The origin of the different frequencies of local power maxima for the two arrays is unclear as the only significant difference between the two array types is the number of load-resistor elements. Just beyond $2f_{op}/3$ for type-A arrays and between $f_{op}/2$ and $2f_{op}/3$ for type-B arrays, we usually observe two stable Shapiro steps in the detector I-V curve. The step heights and voltages (or frequencies f) can be tuned with array bias. For increasing array dc bias, the lower-frequency step height decreases while the higher-frequency step height increases.

Near f_{op}, the height and voltage of a single Shapiro step can be tuned with array bias. The maximum power is observed at f_{op}. The relative bandwidth across which coherent power is observed near f_{op} is ~$0.3f_{op}$. No coherent emission is observed for $f > f_{LC}$. The amplitude of the Shapiro step is not always temporally stable.

Table I: Comparison of P_{det} and P_{th} fo three different arrays with $f_{op} \approx$ 240 GHz. Array A1 has I_c = 23 mA, R = 17.2 mΩ, and R_L = 55.9 Ω. Array B1 has I_c = 23 mA, R = 16.8 mΩ, and R_L = 68.5 Ω . Array B2 has I_c = 17 mA, R = 20.4 mΩ, and R_L = 54.3 Ω.

Array	V_{step} (mV)	f/f_{op}	I_1 (mA)	I_{rf} (mA)	P_{det} (mW)	P_{th} (mW)
A1	0.18	0.38	4	3.9	0.43	*
A1	0.48	1	4.9	5.5	0.85	0.86
A1	0.54	1.13	2.5	2.5	0.18	*
B1	0.24	0.5	5	4.3	0.63	*
B2	0.23	0.46	3.8	3.5	0.33	*
B2	0.50	1	4	4.2	0.49	0.59

Figure 2 shows some detector I-V curves with a variety of array emission. The 5 mA step in Fig. 2a corresponds to I_{rf} = (5.5 ± 0.5) mA; the ±10 % uncertainty in this I_{rf} estimate (and some uncertainty in estimating v_1) mainly arises from uncertainties in β_L and β_c. Table I summarizes data from a number of arrays and modes (including the emission data of Fig. 2). From array A1, for example, the detected power is 0.85 mW, which is 17 times higher than the maximum power from any previously reported array [4].

In order to compare the detected power with the theoretical power P_{th} at f_{op}, Eq. (1), we must estimate R_s^T. We assume that the surface resistance equals 4 mΩ at f = 100 GHz [15] and increases in proportion to f^2. The circuits have $l_{cir}/(84\ \mu m)$ squares. The surface losses are significant: $R_s^T \approx 17\ \Omega$ for array A1 at f_{op}. For $f \neq f_{op}$ (*), we have not estimated p nor P_{th}. Comparison of P_{th} and P_{det} at $f = f_{op}$ in Table I shows that the above-mentioned assumptions give good agreement between P_{th} and P_{det} for array A1, so the array is probably phase locked and in the maximum-p mode.

The arrays of Table I were heat sunk with vacuum grease to Mo and Cu blocks. Some arrays without heat sinking showed a significant decrease of I_c with increasing array bias; for these arrays, $P_{det} < P_{th}$, which is possibly also related to increased R_s^T. When heating reduces I_c by ~50 % (as compared with its 4 K value), the junctions trap flux and the circuits need to be thermally cycled above 9 K.

IV. Conclusions

We have detected power as large as 0.85 mW near 240 GHz. This power agrees with the theoretical power that an array can deliver when spatial modulation of the rf current in the array and conductor losses in the circuit are taken into account. This suggests that this array is phase locked in the maximum-power mode at the operating frequency.

Acknowledgment

We thank R. L. Kautz, G. V. Kunkel, B. H. Larsen, D. G. McDonald, R. H. Ono, and C. D. Reintsema for discussions. P. A. A. Booi acknowledges the support of the University of Twente in The Netherlands.

References

[1] Millitech catalog (1995).
[2] A. K. Jain, K. K. Likharev, J. E. Lukens, and J. E. Sauvageau, Phys. Rep. **109**, 309 (1984).
[3] B. Bi, S. Han, and J. E. Lukens, Appl. Phys. Lett. **62**, 2745 (1993).
[4] S. Han, B. Bi, W. Zhang, and J. E. Lukens, Proceedings of the Fourth ISEC, Boulder, 335 (1993); Appl. Phys. Lett. **64**, 1424 (1994).
[5] S. P. Benz and C. J. Burroughs, Appl. Phys. Lett. **58**, 2162 (1991).
[6] S. P. Benz and C. J. Burroughs, Proceedings of the Third ISEC, Glasgow, 230 (1991); Supercon. Sci. Technol. **4**, 561 (1991).
[7] P. A. A. Booi, S. P. Benz, T. Doderer, D. Hoffmann, J. Schmidt, S. Lachenmann, and R. P. Huebener, IEEE Trans. Appl. Supercon. **3**, 2493 (1993).
[8] P. A. A. Booi and S. P. Benz, Appl. Phys. Lett. **64**, 2163 (1994).
[9] P. A. A. Booi and S. P. Benz, IEEE Trans. Appl. Supercon. **5**, 2899 (1995).
[10] R. F. Miracky, Ph.D. thesis, University of California at Berkeley (1984).
[11] R. L. Kautz, IEEE Trans. Appl. Supercon. **5**, 2702 (1995).
[12] K. Wiesenfeld, S. P. Benz, and P. A. A. Booi, J. Appl. Phys. **76**, 3835 (1994).
[13] P. A. A. Booi and S. P. Benz, submitted to EUCAS'95, Edinburgh (1995).
[14] P. A. A. Booi and S. P. Benz, submitted to Appl. Phys. Lett. (1995).
[15] B. Bi, K. Wan, W. Zhang, S. Han, and J. E. Lukens, IEEE Trans. Appl. Supercon. **1**, 145 (1991).

Fifth
International Superconductive Electronics Conference

September 18 - 21, 1995
Nagoya Congress Center, Nagoya, Japan

EXTENDED ABSTRACTS

Cosponsored by
The Japan Society of Applied Physics
The Institute of Electronics, Information
and Communication Engineering
Aichi Prefecture
Nagoya City